Optical Stern-Gerlach effect from the Zeeman-like ac Stark shift

Chang Yong Park, Ji Young Kim, Jong Min Song, and D. Cho*
Department of Physics, Korea University, Seoul 136-701, Korea
(Received 17 September 2001; published 20 February 2002)

We report a different type of optical Stern-Gerlach effect, where a magnetic-field gradient is replaced with a light-intensity gradient and a paramagnetic atom is deflected according to its magnetic quantum number. The laser light is detuned between the $D1$ and $D2$ frequencies, with the size of the detuning from the $D2$ resonance being twice that from the $D1$ resonance, and it is circularly polarized to produce an ac Stark shift that takes the form of a pure Zeeman shift. Slow rubidium atoms are extracted from a magneto-optical trap and then spin polarized. The atoms traversing the laser-intensity gradient on one side of the Gaussian beam profile show deflections that depend on the atomic spin state and the laser polarization. When the laser-beam axis is aligned with the slit that defines the atomic beam, we observe focusing and defocusing of the atomic beam.

DOI: 10.1103/PhysRevA.65.033410 PACS number(s): 32.80.Lg, 32.60.+i, 32.10.Dk

I. INTRODUCTION

In their landmark experiment of 1922, Stern and Gerlach demonstrated quantization of angular momentum of silver atoms by observing their deflection through a magnetic-field gradient [1]. A similar experiment for a two-level atom with the gradient of a light intensity replacing that of a magnetic field was proposed in the seventies [2]. The experiment was carried out using metastable He atoms in 1992 [3]. The proposal and the experiment were based on a dressed atom picture, where a two-level atom interacting with near-resonant light field forms a pair of atomic eigenstates dressed with photons. Energy eigenvalues of the dressed pair depend on the light intensity in such a way that atoms in orthogonal dressed states experience opposite dipole forces when passing through a light-intensity gradient. Consequent splitting of atomic paths is called the optical Stern-Gerlach effect [4], because it can be thought of as a splitting of a fictitious spin-1/2 system associated with the pair of dressed states.

In this paper we report on an optical Stern-Gerlach effect of a different type. In our work a rubidium atom, which is paramagnetic, passes through a light-intensity gradient, and experiences a deflection proportional to its magnetic quantum number. The experimental situation and interpretation of its result are identical to the original Stern-Gerlach experiment, except that the magnetic field is replaced with a laser field.

The effect is based on the optical dipole force from the Zeeman-like ac Stark shift [5]. The ac Stark shift of an alkali-metal atom in its ground state has contributions from two components, the scalar and vector polarizabilities. It has been known since 1972 that when the light is circularly polarized, the vector-part results in an energy shift analogous to a Zeeman shift [6]. In spite of the widespread use of the dipole force in the field of cooling and trapping of atoms and atom optics, the dipole force from the Zeeman-like ac Stark shift has rarely been used. It may be due to the fact that the vector polarizability is much smaller than the scalar one in most cases of previous studies. We pointed out, however, that when the laser light is detuned between the $D1$ and $D2$ transitions of an alkali-metal atom, the contributions to the vector polarizability from the $D1$ and $D2$ couplings add constructively, while those to the scalar polarizability cancel each other [7]. The magnitude of the vector polarizability in this detuning range is either larger than or comparable to that of the scalar polarizability. There even exists a detuning where the scalar polarizability vanishes and the ac Stark shift becomes identical to the Zeeman shift in its form. For heavy alkali-metal atoms such as rubidium and cesium the fine-structure splitting is large enough to allow the detuning to be far-off resonance from both the $D1$ and $D2$ resonances. This situation was exploited to construct an optical trap that behaved similar to a magnetic trap and held a spin-polarized sample of rubidium atoms [8]. Spin precession of lithium atoms was also demonstrated using a detuning between $D1$ and $D2$ transitions [9].

II. THEORY

The theory of the Zeeman-like ac Stark shift is given in detail in Ref. [7], and here we will summarize the main results only. Suppose an alkali-metal atom in its ground state, $|nS_{1/2},F,m_F\rangle$, where F is the total angular momentum of a hyperfine level, is irradiated by a laser field, $\mathbf{E}(t)=\mathcal{E}_0 e^{-i\omega t}+\mathcal{E}_0^* e^{i\omega t}$, propagating along the z axis. Its ac Stark shift is

$$U(nS_{1/2},F,m_F)=[\alpha+i\beta g_F m_F(\hat{\varepsilon}^*\times\hat{\varepsilon})\cdot\hat{z}]|\mathcal{E}_0|^2, \tag{2.1}$$

where α and β are the scalar and vector polarizabilities, respectively, g_F is the Lande g factor, and $\hat{\varepsilon}$ is a unit vector representing the laser polarization. When the laser is tuned near the alkali-metal D transitions, the scalar and vector polarizabilities take the approximate forms of

$$\alpha(\omega)\simeq\frac{|\langle nS_{1/2}|er|nP_{1/2}\rangle|^2}{9}\left[\frac{1}{\Delta_{1/2}}+\frac{2}{\Delta_{3/2}}\right], \tag{2.2}$$

$$\beta(\omega)\simeq\frac{|\langle nS_{1/2}|er|nP_{1/2}\rangle|^2}{9}\left[\frac{1}{\Delta_{1/2}}-\frac{1}{\Delta_{3/2}}\right]. \tag{2.3}$$

*Email address: cho@korea.ac.kr

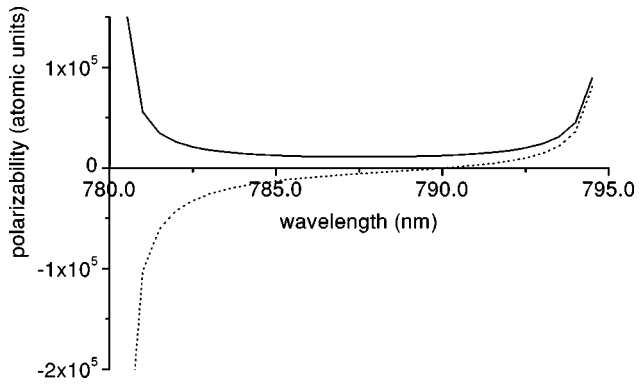

FIG. 1. Scalar polarizability α (dotted line) and vector polarizability β (solid line) of rubidium in atomic units for wavelength between the $D1$ and $D2$ resonances.

Here $\Delta_{1/2}=\hbar\omega-(E_{nP_{1/2}}-E_{nS_{1/2}})$ and $\Delta_{3/2}=\hbar\omega-(E_{nP_{3/2}}-E_{nS_{1/2}})$. Figure 1 shows α and β for rubidium in atomic units between the $D1$ and $D2$ resonances. We note that when $\Delta_{3/2}=-2\Delta_{1/2}$ ($\lambda=790$ nm) α vanishes. When the laser is right circularly polarized,

$$U(nS_{1/2},F,m_F)=-\beta(\omega)|\mathcal{E}_0|^2 g_F m_F, \tag{2.4}$$

i.e., the ac Stark shift takes the form of a pure Zeeman shift. The effective magnetic field is along the direction of the laser propagation and its magnitude is $\beta|\mathcal{E}_0|^2/\mu_B$ with μ_B being the Bohr magneton. The effective field can be either parallel or antiparallel to the laser propagation depending on the light helicity. When 1 W of laser power is focused to a spot size of 10 μm, the effective magnetic field at the focus is 250 G.

III. APPARATUS

The apparatus is outlined in Fig. 2. It consists of an atomic-beam source, the spin-polarization region (A), the interaction region (C), where the optical Stern-Gerlach effect takes place, and finally the probe region (B) where the transverse displacement is measured. The A and C regions are separated by a vertical slit.

In the C region, a vertically propagating (z axis) Gaussian laser beam, which we will call the Stern-Gerlach beam, is tightly focused right at the exit of the vertical slit. Its minimum spot size is ω_0 (e^{-2} intensity radius) and its propagation axis is off from the slit center by y_C. An atom traveling along the x axis through the slit center with the velocity v_x encounters the Stern-Gerlach beam with an impact parameter y_C, and it experiences an impulse along the y axis. After a free flight of distance L from the C to B region, it hits the detector at y_B. Using the impulse approximation and Eq. (2.4) we find the transverse displacement y_B to be

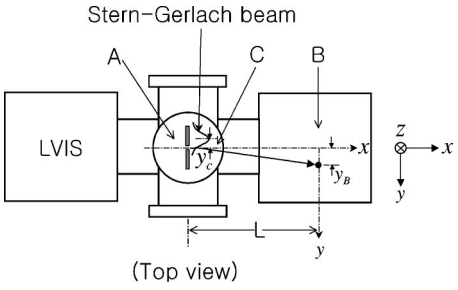

FIG. 2. Outline of the apparatus. The Stern-Gerlach beam is propagating into the page. Its Gaussian intensity profile in the xy plane is shown as a Gaussian curve.

$$y_B=\sqrt{\frac{8}{\pi}}\frac{\beta(\omega)g_F m_F PL}{c\epsilon_o\omega_0^2 m v_x^2} f(y_C/\omega_0), \tag{3.1}$$

where P is the laser power, m is the atomic mass, and $f(x)=xe^{-2x^2}$. The function $f(x)$ has a maximum $1/\sqrt{4e}$ at $x=\pm 1/2$, or when the impact parameter is half the spot size.

For a rubidium atom, when α vanishes, $\beta\simeq 1.2\times 10^4$. In the experiment we use $P=2$ W, $\omega_0=28$ μm, and $L=0.1$ m. The width of the slit is 10 μm. If we use an effusive oven source with a typical beam velocity of 300 m/s, our apparatus parameters would produce the maximum transverse displacement y_B of less than 1 μm. In order to take advantage of the $1/v_x^2$ dependence of y_B we employ a slow atomic beam extracted from a magneto-optical trap (MOT) through a 2-mm diameter hole on one of its optics. This type of beam source was developed by Lu *et al.* [10], and it is called a low-velocity intense source (LVIS). Its longitudinal beam velocity is around 15 m/s, and the expected maximum y_B is 290 μm. Our LVIS setup uses standard ultrahigh vacuum components with rubidium getters and external-cavity diode lasers. It is described in Ref. [11]. We operate it in a pulsed mode at 2 Hz. There are a few times 10^7 atoms per pulse.

In the probe region rubidium atoms are detected by surface ionization on a 50-μm diameter platinum/iridium hot wire. The resulting ions are collected and multiplied by a channel electron multiplier (CEM). The detector assembly of the hot wire and the CEM is translated along the y axis by a stepper motor. The background counting rate is typically less than 1 kHz. After a few hours of running the beam source, however, the rubidium vapor pressure in the detector chamber goes up, and the background can be as high as 3 kHz. The pulsed operation of the LVIS allows us to improve the signal-to-background ratio; we integrate the digitized CEM output for only 100 ms to detect atoms collected in a MOT during 400 ms.

IV. MEASUREMENT AND RESULT

Spin-polarization method employed in the experiment selects the atoms in the lower hyperfine level of the $5S_{1/2}$ state. Specifically, the Zeeman states with $m_F=\pm F$ are used for the measurement. For these stretched states, $|g_F m_F|$ of ^{85}Rb is 2/3, while that of ^{87}Rb is 1/2. Because the transverse displacement, Eq. (3.1), is proportional to $|g_F m_F|$, and ^{85}Rb is more abundant, we use ^{85}Rb for the measurement.

One drawback of the original LVIS is that its beam is rather divergent [10]. With the 10-μm wide slit in place, there were very few atoms reaching the hot wire, and we had considerable difficulty in detecting them with a high enough

signal-to-noise ratio. We modified the LVIS design and introduced an extra push beam whose frequency, intensity, mode, and polarization could be controlled independently from the MOT trapping light. With careful optimization of the parameters we obtain significant improvement in the collimation at the expense of only a slight increase in the longitudinal velocity. A detailed account of the design and its performance is given elsewhere [12]. With the modified LVIS, when the beam is unobstructed, we detect 10^4 ions per LVIS pulse. With the slit in, the ion signal, when the hot wire is aligned to the slit, is 500. From the time-of-flight measurement we estimate the longitudinal velocity to be around 20 m/s.

When atoms are allowed to fly freely through the slit, the full width at half maximum of the ion signal for a hot-wire scan along the y axis is 400 μm. It is undesirably large considering that the expected transverse displacement y_B due to the optical Stern-Gerlach effect is only 140 μm for $v_x = 20$ m/s. The width is comparable to the size of a MOT, and it appears that the scan result represents an image of the MOT through the slit, as in a pin-hole camera. When we replace the 10-μm slit with a 50-μm slit, the signal becomes much bigger, but the width remains almost the same. In addition, the horizontal position of the ion-signal maximum is very sensitive to the LVIS B field, which determines the position of the MOT center. We could have reduced the width by adding another slit along the beam path, but that would have made the signal size prohibitively small.

In the A region, just upstream of the slit, we spin polarize the atoms. Normally one would use optical pumping to put the atoms in a well-defined hyperfine and Zeeman sublevel. In our experiment, however, the expected impulse from the optical Stern-Gerlach effect is comparable to that of six-photon recoils. We cannot afford to bombard the atoms with resonant photons just before the narrow collimating slit. As a result, instead of ''flipping in'' the atoms to the state of interest by optical pumping, we ''flop off'' the atoms in the wrong states by ''optical kicking.'' In our measurement the state of interest is $|5S_{1/2},F=2,m_F=2\rangle$, and the quantization axis is defined by a magnetic field **B** along the z axis of the vertical direction. For the optical kicking we employ two laser beams propagating along the z axis. One is tuned to the cycling transition, from $|5S_{1/2},F=3\rangle$ to $|5P_{3/2},F=4\rangle$, and we call it the cycling beam. It has ten times the saturation intensity and pushes away all the atoms in the upper hyperfine state. The other is tuned to the transition from the $|5S_{1/2},F=2\rangle$ to the $|5P_{3/2},F=2\rangle$ state, and we call it the Zeeman pumping beam. It is right circularly polarized, and puts all the atoms in the lower hyperfine state except $|5S_{1/2},F=2,m_F=2\rangle$ via optical pumping into $|5S_{1/2},F=3\rangle$ state as shown in Fig. 3. Once pumped into the $|5S_{1/2},F=3\rangle$ state, atoms are pushed away by the cycling beam. The $|5S_{1/2},F=2,m_F=2\rangle$ state is a dark state for the Zeeman pumping beam, and only the atoms in the state survive the optical kicking.

We first null out the stray field in the A region originating from the anti-Helmholtz coil for the LVIS by using shim coils. We then apply an 8 G magnetic field **B** along the z axis. When the cycling beam is applied in the A region, the ion

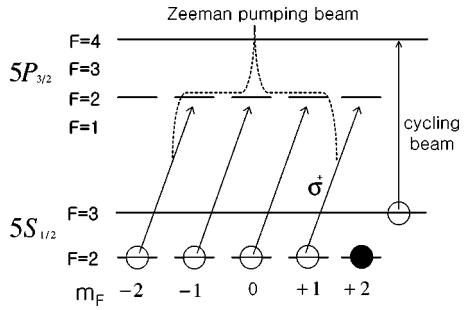

FIG. 3. ''Optical-kicking'' scheme. The cycling beam tuned to the cycling transition and circularly polarized Zeeman pumping beam can push away all atoms except those in the $|5S_{1/2}, F=2, m_F=2\rangle$ state. The dashed line is to indicate the transitions driven by the Zeeman pumping beam.

signal from the hot-wire detected atoms drops by only 25% due to the deflection of atoms in the upper hyperfine state. This small value implies that the LVIS beam has a highly nonthermal population distribution. The push beam, tuned close to the cycling transition, optically pumps the atoms into the lower hyperfine state as well as pushing them out of LVIS. Next we apply the Zeeman pumping beam. We keep its intensity far below saturation to avoid off-resonant excitation from power broadening. The ion signal resulting from atoms that survive the optical kicking versus the polarization of the Zeeman pumping beam is shown in Fig. 4. We note that the ion signal exhibits a minimum when the Zeeman pumping beam is linearly polarized ($\theta=0$), and that it shows two asymmetric peaks at the right and left circular polarizations. The peaks represent the surviving atoms in either the $|5S_{1/2},F=2,m_F=+2\rangle$ state or the $|5S_{1/2},F=2,m_F=-2\rangle$ state. The asymmetry is also a result of the optical pumping effect of the LVIS push beam, which is circularly polarized. The ion-signal curve obtained with the magnetic field **B** in the A region reversed is a reflection of the original one with respect to $\theta=0$. It implies that the atomic spin follows the local magnetic-field adiabatically through the beam machine. For the curves in Fig. 4 we tune the Zeeman pumping laser to the resonance of the $|5S_{1/2},F=2\rangle$ to $|5P_{3/2},F=2\rangle$ transition. Due to the Zeeman shift induced by **B**, the shape of the ion-signal curve changes depending on the detuning of

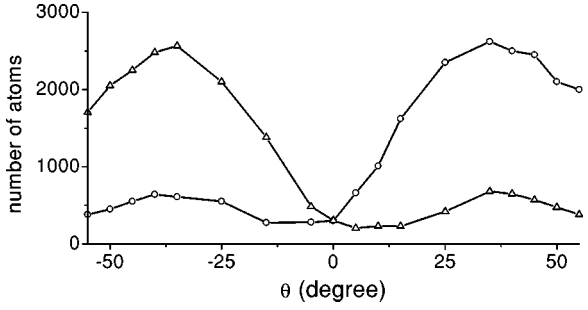

FIG. 4. Number of atoms surviving the optical kicking vs the Zeeman pumping-beam polarization. θ is the angle of a quarter wave plate with $\theta=0$ producing a linear polarization. ○ is when the magnetic field **B** is parallel to the z axis and △ is when **B** is antiparallel.

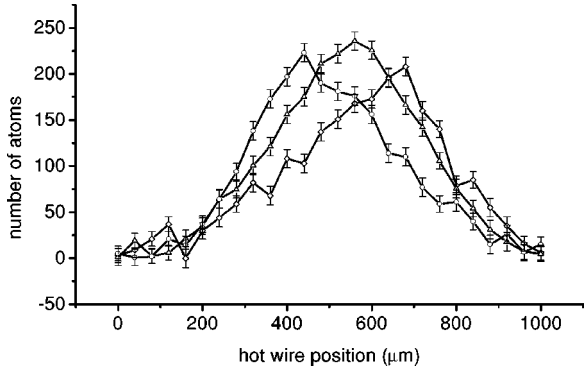

FIG. 5. Hot-wire scan results. Scan 1 (△) is when the Stern-Gerlach beam is blocked. Scan 2 (○) and 3 (◇) are when the Stern-Gerlach beam is turned on and right and left circularly polarized, respectively.

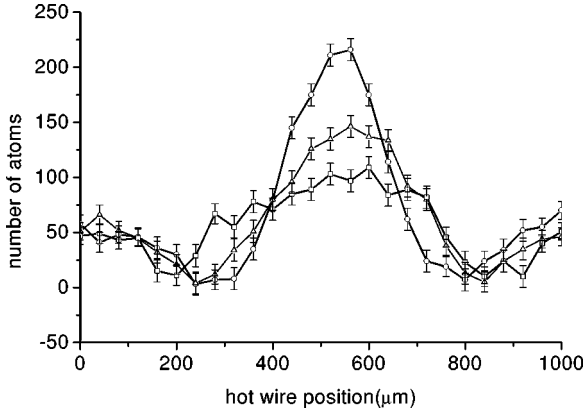

FIG. 6. Focusing and defocusing of the atomic beam due to the optical Stern-Gerlach effect. Scan 1 (△) is when the Stern-Gerlach beam is blocked. Scan 2 (○) and 3 (◇) are taken when the Stern-Gerlach beam is aligned with the slit and right and left circularly polarized, respectively.

the Zeeman pumping beam. We use the detuning that produces the biggest contrast between the two peaks. When the laser is 15 MHz blue detuned from the resonance, the contrast is 6 to 1, and we have 40% of the total atoms in the large peak. However, we do not know the exact population distribution of the surviving atoms among the Zeeman sublevels. We only know that the distribution is highly skewed and that the atoms with m_F of one sign is larger than the other by a factor of the order of the contrast factor.

In the *C* region, 3 mm downstream of the slit, we focus a 2-W Stern-Gerlach beam from a free-running Ti:sapphire laser to a spot with $\omega_0 = 28\ \mu$m. Figure 5 shows the results of hot-wire scans when the laser spot is positioned for maximum transverse deflection of atoms. The step size of the scan is 40 μm, and for each data point, 30 LVIS pulses are averaged. Scan 1 (△) in the figure is when the Stern-Gerlach beam is blocked, and the atoms travel freely. When the Stern-Gerlach beam at 790 nm is turned on with linear polarization, the scan result is virtually identical to the scan 1 within measurement error. It is not shown in Fig. 5. Scan 2 (○) and scan 3 (◇) are the results with the Stern-Gerlach beam right and left circularly polarized, respectively. They have peaks shifted from the free one by $\pm 125\ \mu$m in reasonable agreement with Eq. (3.1). The skewness of the curves is the result of both incomplete atomic spin polarization and a distribution of impact parameter y_C due to the width of the atomic-beam profile defined by the slit. From the atomic-beam divergence and the slit to spot distance, we estimate the beam width at the impact plane to be comparable to ω_o. At 790 nm and for the given intensity, atoms in the atomic beam scatter a negligible number of Stern-Gerlach beam photons.

When we reverse the magnetic field **B** in the *A* region, we obtain the same result as those in Fig. 5 except that the roles of the right and the left circular polarizations of the Stern-Gerlach beam are interchanged. Finally, we move the Stern-Gerlach beam along *y* direction so that its axis is aligned with the slit center ($y_C = 0$ in Fig. 2). The scan results are shown in Fig. 6, and again the linear polarization (△) produces the same result as the free flight. With the right (○) and the left circular (◇) polarizations we clearly see the focusing and defocusing effects, respectively, of the Stern-Gerlach beam. The focal length can be varied by changing the laser power. The data in Fig. 6 is taken when the power is 1.42 W.

V. CONCLUSION

While the optical Stern-Gerlach effect in previous studies can be understood only by invoking a fictitious spin 1/2 associated with a two-level system, the present work demonstrates the Stern-Gerlach effect on a paramagnetic atom by simply using a light field in place of a magnetic field. Since a laser beam can be tightly focused with lenses, made into a standing wave, and used for optical pumping, the laser-induced Stern-Gerlach force provides a versatile tool in optically manipulating atomic motion in a spin-dependent way. As a byproduct we also developed a method of producing a slow atomic beam from a magneto-optical trap with better control on its velocity and population distributions.

ACKNOWLEDGMENT

This work was supported by the Ministry of Education (Grant No. 1998-001-D00253).

[1] W. Gerlach and O. Stern, Z. Phys. **8**, 110 (1922).

[2] A.P. Kazantsev, Zh. Éksp. Teor. Fiz. **67**, 1660 (1975) [Sov. Phys. JETP **40**, 825 (1075)].

[3] T. Sleator, T. Pfau, V. Balykin, O. Carnal, and J. Mlynek, Phys. Rev. Lett. **68**, 1996 (1992).

[4] D. F. Walls and G. J. Milburn, *Quantum Optics* (Springer-Verlag, Berlin, 1994).

[5] Chang Yong Park, Heeso Noh, Chung Mok Lee, and D. Cho,

Phys. Rev. A **63**, 032512 (2001).

[6] C. Cohen-Tannoudji and J. Dupont-Roc, Phys. Rev. A **5**, 968 (1972).

[7] D. Cho, J. Korean Phys. Soc. **30**, 373 (1997).

[8] K.L. Corwin, S.J.M. Kuppens, D. Cho, and C.E. Wieman, Phys. Rev. Lett. **83**, 1311 (1999).

[9] M. Zielonkowski, J. Steiger, U. Schunemann, M. DeKieviet, and R. Grimm, Phys. Rev. A **58**, 3993 (1998).

[10] Z.T. Lu, K.L. Corwin, M.J. Renn, M.H. Anderson, E.A. Cornell, and C.E. Wieman, Phys. Rev. Lett. **77**, 3331 (1996).

[11] M.S. Jun, C.Y. Park, and D. Cho, J. Korean Phys. Soc. **33**, 260 (1998).

[12] Chang Yong Park, Ph.D. thesis, Korea University, 2002.